PHYSICAL REVIEW B **90**, 121113(R) (2014)

Soft striped magnetic fluctuations competing with superconductivity in $Fe_{1+x}Te$

C. Stock,[1] E. E. Rodriguez,[2] O. Sobolev,[3] J. A. Rodriguez-Rivera,[4,5] R. A. Ewings,[6] J. W. Taylor,[6] A. D. Christianson,[7] and M. A. Green[8]

[1]*School of Physics and Astronomy, University of Edinburgh, Edinburgh EH9 3JZ, United Kingdom*
[2]*Department of Chemistry and Biochemistry, University of Maryland, College Park, Maryland, 20742, USA*
[3]*Forschungs-Neutronenquelle Heinz Maier-Leibnitz, FRM2 Garching, 85747, Germany*
[4]*NIST Center for Neutron Research, National Institute of Standards and Technology, 100 Bureau Dr., Gaithersburg, Maryland 20889, USA*
[5]*Department of Materials Science, University of Maryland, College Park, Maryland 20742, USA*
[6]*ISIS Facility, Rutherford Appleton Laboratory, Didcot, OX11 0QX, United Kingdom*
[7]*Quantum Condensed Matter Division, Oak Ridge National Laboratory, Oak Ridge, Tennessee 37831, USA*
[8]*School of Physical Sciences, University of Kent, Canterbury, CT2 7NH, United Kingdom*

(Received 6 January 2014; revised manuscript received 9 September 2014; published 30 September 2014)

Neutron spectroscopy is used to investigate the magnetic fluctuations in $Fe_{1+x}Te$—a parent compound of chalcogenide superconductors. Incommensurate "stripelike" excitations soften with increased interstitial iron concentration. The energy crossover from incommensurate to stripy fluctuations defines an apparent hourglass dispersion. Application of sum rules of neutron scattering find that the integrated intensity is inconsistent with an $S = 1$ Fe^{2+} ground state and significantly less than $S = 2$ predicted from weak crystal field arguments pointing towards the Fe^{2+} being in a superposition of orbital states. The results suggest that a highly anisotropic order competes with superconductivity in chalcogenide systems.

DOI: 10.1103/PhysRevB.90.121113 PACS number(s): 74.25.Ha, 74.70.−b, 78.70.Nx

Pnictide and chalcogenide superconductors have altered the view of what provides the basis for high temperature superconductivity. While the cuprate superconductors universally derive from Mott insulators which can, at least qualitatively, be understood in terms of a single electronic band, the parent phase of iron-based superconductors has been less clear: Fe-based parent phases are either poorly metallic or semimetallic resulting in a debate over whether a localized or itinerant/spin-density-wave picture is more appropriate [1,2]. Towards this goal, it is important to understand the magnetic excitation spectrum in starting materials as superconducting variants consist of fluctuating versions of this ground state [3]. Here we study $Fe_{1+x}Te$ which is arguably the structurally simplest of the iron superconductors based upon single layers of tetrahedrally coordinated Fe^{2+} ions [4,5]. While the iron superconductors have been shown to display both localized [6,7] and itinerant properties [8,9], $Fe_{1+x}Te$ hosts one of the most localized responses of all iron-based superconductors evidenced by large ordered magnetic moments and calculated heavy band masses [10].

In this study, we combine neutron scattering data from spectrometers with overlapping dynamic ranges on two samples of $Fe_{1+x}Te$ to understand the magnetic fluctuations. We report a one-dimensional incommensurate excitation that softens with increased charge doping with interstitial iron and hence competes with unconventional chalcogenide superconductivity. We apply sum rules of neutron scattering to evaluate the spin and orbital ground state of the iron cations. The results represent a dynamical signature of a highly anisotropic striped order which competes with superconductivity in the chalcogenides.

Superconductivity in $Fe_{1+x}Te_{1-y}Ch_y$ (where Ch is a chalcogenide ion) has been most commonly achieved through anion substitution on the Te site y with either sulfur or selenium [11,12]. However, the cation concentration (interstitial iron x) in $Fe_{1+x}Te_{1-y}Ch_y$ is directly correlated with the anion concentration (y) and chemical techniques have been developed to independently tune x and y [13]. Several studies have found that changing the concentration of interstitial iron has analogous effects to anion doping for a fixed selenium concentration [14–16].

The structural and magnetic properties of $Fe_{1+x}Te$ as a function of x have been reported by several groups giving generally consistent results [17–21]. A neutron diffraction study found a phase diagram with two distinct phases as a function of interstitial iron [22]. For low concentrations of $x < 11\%$, a commensurate collinear magnetic phase is realized with the critical properties being first order. For large $x > 11\%$, the transition is second order with a spiral magnetic low-temperature phase. The two extremes are separated by a tricritical-like point at $x \sim 11\%$ where short-range incommensurate spin-density wave order is observed. Resistivity measurements found the collinear $x < 11\%$ values to be metallic at low temperatures while larger $x > 11\%$ are "semi" (or poorly) metallic and scattering from incommensurate spin fluctuations was implicated as the origin of the enhanced resistivity [23]. Therefore, based upon the fixed selenium studies [15,16] and these magnetic and structural results, metallicity and superconductivity are favored for smaller values of interstitial iron.

Doping charge through interstitial iron therefore remains an independent means of controlling the electrical properties of the chalcogenides. We present neutron inelastic data taken from steady state reactor sources (MACS, PUMA, and HB1) and time-of-flight instruments (MAPS) based at pulsed spallation sources. Further experimental and sample details are given in the Supplemental Material [24] (see also Ref. [25]) and also details on phonon contamination and how these were disentangled (see also Ref. [26]).

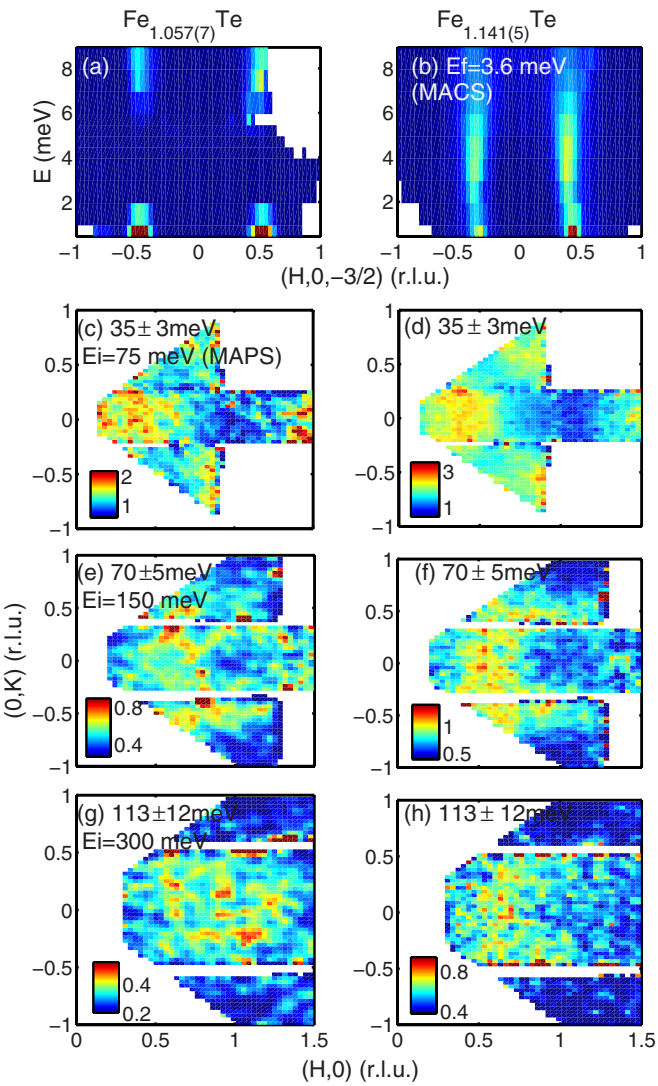

FIG. 1. (Color online) Neutron inelastic scattering comparing commensurate $Fe_{1.057(7)}Te$ with incommensurate $Fe_{1.141(5)}Te$. (a), (b) Constant-Q slices of the low-energy data taken on MACS (E_f = 2.6 meV). (c)–(h) Constant energy slices from MAPS taken with incident energies of 75, 150, and 350 meV.

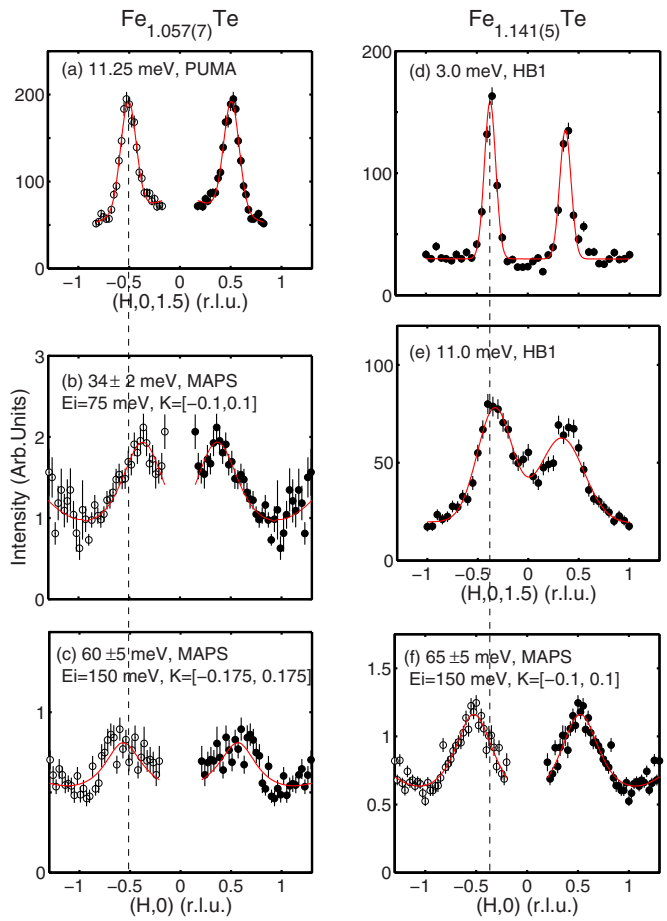

FIG. 2. (Color online) Cuts along the $(H,0)$ direction for commensurate $x = 0.057(7)$ (a)–(c) and incommensurate $x = 0.141(5)$ (d)–(f) crystals. The data is taken from thermal triple-axis and spallation source data. Open circles are symmetrized data and displayed for visual comparison.

We first describe the dispersion of the spin excitations in momentum. Representative constant energy and momentum slices are displayed in Fig. 1 for both interstitial iron concentrations. Panels (a) and (b) show high-energy resolution constant-Q slices illustrating the gapped nature of the excitations for collinearly ordered $x = 0.057(7)$ and the gapless low-energy incommensurate fluctuations for $x = 0.141(5)$ in the spiral magnetic phase [27]. Higher-energy excitations are displayed in panels (c)–(h) through a series of constant energy slices at 35, 70, and 113 meV. The data do not show clean circular spin-wave cones, but rather excitations broad in momentum and dispersing to the zone boundary.

Constant energy cuts for both commensurate and incommensurate crystals are presented in Fig. 2. The solid lines are fits to a Gaussian line shape multiplied by the isotropic Fe^{2+} form factor squared [28] from which a peak position and integrated intensity were derived. The open symbols are symmetrized data around $\vec{Q} = 0$. The vertical dashed lines emphasize the fact that as the energy transfer is increased, the peak position in momentum disperses inward and then outward at higher energies.

Based upon fits (Fig. 2) we construct a dispersion curve (Fig. 3) along the [1,0] direction comparing the commensurate and incommensurate crystals. For the commensurate $x = 0.057(7)$ sample, the excitations are gapped (Fig. 1) and then disperse inwards to a wave vector $H \leqslant 0.4$ at around 30 meV energy transfer. The excitations then disperse towards the zone boundary which is reached at ∼100 meV. Interestingly, the excitations are nearly vertical as they extend to higher energies indicative of strong dampening at the zone boundary. This marks a clear distinction from predictions based upon a localized Heisenberg exchange [29]. A strong zone boundary dampening has been reported in superconducting iron-based variants [30], in cuprates and associated with the onset of the electronic pseudogap [31], and predicted to exist in Cr metal [32]. Our results, however, mark a clear difference between parent cuprates (and even cuprates close to the charged doped boundary of superconductivity) [33,34] and iron-based systems as we do not see localized spin waves

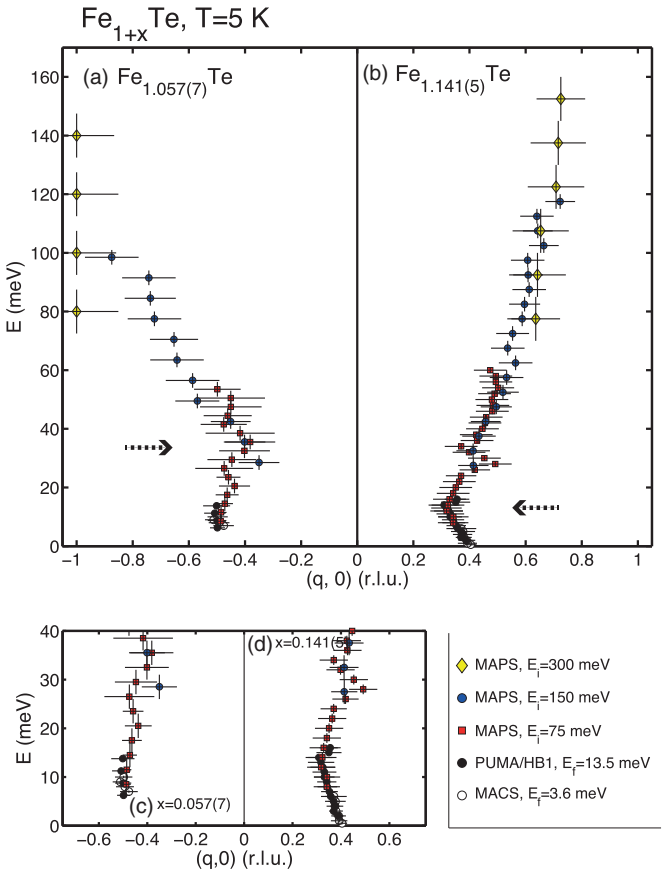

FIG. 3. (Color online) The dispersion of the magnetic excitations in $Fe_{1+x}Te$ with $x = 0.057(7)$ (a) and $x = 0.141(5)$ (b) representative of commensurate and incommensurate magnetically ordered phases, respectively. (c) and (d) show the low-energy portion of the magnetic dispersion. The data is a compilation of triple-axis and spallation data. The inward dispersion described in the text is highlighted by the arrows.

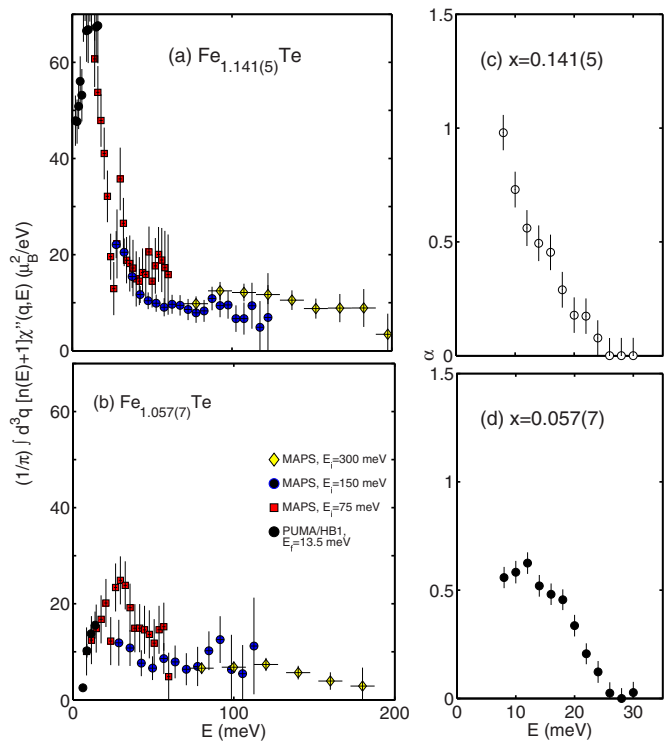

FIG. 4. (Color online) Momentum integrated intensity in absolute units as a function of energy transfer for (a) incommensurate $x = 0.141(5)$ and (b) commensurate $x = 0.057(7)$ samples. The "stripe" correlation parameter α is plotted for both concentrations in (c) and (d).

which can be interpreted in terms of a localized Heisenberg model on a Mott insulating ground state.

The fluctuations in incommensurate $x = 0.141(5)$ are different. The low-energy fluctuations are gapless and disperse inwards until ~20 meV and then disperse outwards until the highest energy transfers studied. However, in contrast to the commensurate $x = 0.057(7)$ material the excitations do not reach the zone boundary but disperse up to the highest energies studied. There are therefore two effects of doping with interstitial iron—first, to decrease or soften the inward dispersing minimum in the magnetic excitations, and second, to increase the top of the excitation band. A common feature from both interstitial iron concentrations is the inward (or nearly vertical) dispersion at low energies. This dispersion never reaches the commensurate $Q = 0$ positions, but disperses towards an incommensurate position that softens in energy with increased interstitial iron concentration.

The energy inward dispersion in Fig. 3 also represents a crossover from two-dimensional excitations to strongly one-dimensional where the momentum dependence is well defined in H, however broad along both L and K. This is illustrated in Fig. 1(f) that shows the magnetic fluctuations form stripes at high energy. To characterize this, we have fit the K dependence at each energy transfer to $I(K) \propto (1 + 2\alpha \cos[\vec{Q} \cdot \vec{b}])$, where α represents the strength of correlations between stripes aligned along a. The results are shown in Figs. 4(c) and 4(d) for both interstitial iron concentrations. The parameter α falls, within error, to zero at energies above the inward dispersion indicating one-dimensional stripy fluctuations—a feature absent in superconducting chalcogenides [30] and pnictides [35–37]. The highly one-dimensional nature of the fluctuations indicates that a highly anisotropic order is proximate in the chalcogenide superconductors. The anisotropy exceeds that observed in superconducting LaFeAsO [38] and $CaFe_2As_2$ in the paramagnetic phase [39]. While the the results may indicate stripelike fluctuations, as discussed in the context of the cuprates [40,41], it may also reflect an underlying anisotropy associated with the orbital ground state. It is difficult to interpret the results in terms of anisotropic localized exchange (as recently done for the low-energy fluctuations $K_{0.85}Fe_{1.54}Se_2$ [42] and $SrCo_2As_2$ [43]) given the lack of spin-wave cones and the integrated intensity discussed below. Highly anisotropic orders such as quadruopolar order, discussed in terms of triangular $S = 1$ magnets originating from biquadratic exchange (term "spin nematic") [44,45], or "nematic" order connected with the underlying Fermi surface topology may be the origin [46–49]. We note that all of these proposals predict a director where, in analogy to liquid crystals, there is some form of orientational order.

To understand the underlying ground state, we now discuss the integrated intensities. The $\vec{q}$ integrated intensity for the commensurate and incommensurate samples is shown in Fig. 4. The calibration method is discussed in the Supplemental Material (see also Refs. [50–54]). The integrated intensity shows a peak near where the momentum dispersion (Fig. 3) shows a minimum in wave vector reflecting a Van Hove–type singularity where the group velocity of the magnetic mode reaches zero. For both interstitial concentrations at large energy transfers above the peak in the local susceptibility, the integrated intensity is nearly constant. The average value at these energy transfers is similar to the normalized values reported for pnictide systems such as $CaFe_2As_2$ [36] indicating a strong similarity in the physics between the pnictides and the chalcogenides.

The combined inward dispersion and peak in the local susceptibility indicate an hourglasslike dispersion. While similar to $La_{2-x}Sr_xCuO_4$, the momentum dependence in $Fe_{1+x}Te$ differs to $YBa_2Cu_3O_{6+x}$ where the two branches meet at the commensurate (π,π) point [55–58]. Similar structures have also been observed in more localized $La_{5/3}Sr_{1/3}CoO_4$ [59] and single-layered manganites [60]. Interestingly, the hourglass dispersion is absent in the superconducting state $Fe_{1+x}Te_{0.7}Se_{0.3}$ [61]. An analogous "U"-type dispersion was observed to be stabilized by Ni/Cu doping [62] which suppressed superconductivity and incommensurate order has been observed near the superconducting phase in $BaFe_{2-x}Ni_xAs_2$ and $Fe_{1+x}Se_yTe_{1-y}$ [63,64]. These results indicate that the soft incommensurate mode is detrimental to superconductivity and, given the presence in both localized and metallic magnets, that the hourglass dispersion is not directly tied to an electronic origin. Our results would point towards the hourglass point marking a crossover from two-dimensional to one-dimensional fluctuations as discussed above.

Based on the available magnetic and crystal field data, it is not clear how to understand the single-ion properties of the tetrahedrally coordinated Fe^{2+} ion in $Fe_{1+x}Te$. Hence the neutron scattering cross section, which is typically fixed by the value of S, is uncertain. In a localized model, there are two possible scenarios for populating the $3d^6$ electron configuration [6,65]. In the the first case, termed the weak or intermediate crystal field limit, Hund's energy scale dominates and the low-energy doubly degenerate $|e\rangle$ and higher-energy triply degenerate $|t\rangle$ states are populated giving $S = 2$. At the other extreme, referred to as the large crystal field limit, the energy splitting between $|e\rangle$ and $|t\rangle$ dominates and this results in an orbital triplet state with $S = 1$ [66]. An interplay between these two energy scales has been suggested to cause a possible spin-state transition in pnictides [67]. $Fe_{1+x}Te$ has been argued to be in this strong crystal field $S = 1$ limit [68,69]. This also seems to be corroborated by a series of neutron diffraction results in the chalcogenide and pnictide systems where small ordered (proportional gS, where g is the Landé factor) moments are reported.

The neutron scattering cross section is governed by several sum rules, and in particular the zeroth moment sum rule which can be written as $\int dE \int d^3q \frac{1}{\pi}[n(E)+1]\chi''(q,E) = \frac{1}{3}g^2\mu_B^2 S(S+1)$ (further details are provided in the Supplemental Material). The integral includes both elastic and inelastic scattering contributions and is independent of broadening due to itinerant effects as the integral is performed over all momentum and energy. Some estimates on the value for S have been made based upon purely localized spin-wave models as in $CaFe_2As_2$ [36] and $BaFe_2As_2$ [70]. These have been summarized for other 122 systems and are typically in the range from $S\sim0.4$–1 [71]. Pure FeAs has an ordered spiral magnetic moment of only $0.5\mu_B$ with no dynamics reported [72]. These small values are consistent with a strong crystal field picture fixing $S = 1$. However, we also note that neutron inelastic scattering results on Mott insulating $La_2O_2Fe_2OSe_2$ have been consistent with the weak crystal field picture with $S = 2$ [73–75] and the large ordered moments in $K_xFe_{2-y}Se_2$ variants [76].

Through the use of the total moment sum rule we can estimate S in $Fe_{1+x}Te$. As we have noted, while our results which extend up to energy transfers of 175 meV do not capture all of the magnetic cross section, an integral over this energy range gives a lower limit on the total spectral weight and hence an effective S. Combining both static and dynamic contributions gives $3.4 \pm 0.3\mu_B^2$ and $3.7 \pm 0.3\mu_B^2$ for $x = 0.141(5)$ and $0.057(7)$, respectively. For $S = 1$ and 2 we would expect a total integral of 2.67 and $8\mu_B^2$, respectively. Entropic arguments based upon high-temperature heat capacity measurements would suggest that $S_{\text{eff}} = \frac{3}{2}$ is more appropriate and this would give a predicted integral of $5\mu_B^2$, closer to our measurements given that even at 175 meV the top of the band has not been reached. While our results are consistent with earlier low-energy measurements on $Fe_{1.11}Te$ [77], we find significant spectral weight extending up to high energies giving the apparent low-temperature discrepancy. More discussion on this point is provided in the Supplemental Material. The integrated intensities are difficult to understand in terms of a purely localized model with $S = 1$ or 2 discussed above, therefore suggesting the importance of itinerant effects. Such effects may be captured by considering orbital transitions [78] or an orbitally entangled ground state which can also account for the highly anisotropic nature suggested by the high-energy spin dynamics [79]. We have searched for high-energy orbital transitions without success and this is discussed in the Supplemental Material (see also Refs. [80–84]).

In summary, our work finds three results based upon our study of the spin fluctuations in parent $Fe_{1+x}Te$. First, we observe the presence of a soft incommensurate stripy excitation. Second, by applying sum rules, we find the integrated intensity to be inconsistent with an $S = 1$ ground state expected in the presence of a strong crystalline electric field. Third, our results produce an apparent hourglass structure which defines a crossover point from two-dimensional fluctuations to one dimensional. The results point to the parent Fe^{2+} ground state of chalcogenide superconductors being highly anisotropic and also in an intermediate state between strong ($S = 2$) and weak ($S = 1$) orbital ground states.

We are grateful for funding from the Royal Society of Edinburgh, the Carnegie Trust for the Universities of Scotland, STFC, and through the National Science Foundation (Grant No. DMR-09447720).

[1] D. C. Johnston, Adv. Phys. **59**, 803 (2010).
[2] R. J. Birgeneau, C. Stock, J. M. Tranquada, and K. Yamada, J. Phys. Soc. Jpn. **75**, 111003 (2006).
[3] P. A. Lee, N. Nagaosa, and X. G. Wen, Rev. Mod. Phys. **78**, 17 (2006).
[4] D. Fruchart, P. Convert, P. Wolfers, R. Madar, J. P. Senateur, and R. Fruchart, Mater. Res. Bull. **10**, 169 (1975).
[5] F. C. Hsu, J. Y. Luo, K. W. Yeh, T. K. Chen, T. W. Huang, P. M. Wu, Y. C. Lee, Y.-L. Huang, Y. Y. Chu, D. C. Yan, and M. K. Wu, Proc. Natl. Acad. Sci. USA **105**, 14262 (2008).
[6] Q. Si and E. Abrahams, Phys. Rev. Lett. **101**, 076401 (2008).
[7] D. X. Yao and E. W. Carlson, Phys. Rev. B **78**, 052507 (2008).
[8] I. I. Mazin, D. J. Singh, M. D. Johannes, and M. H. Du, Phys. Rev. Lett. **101**, 057003 (2008).
[9] K. Kuroki, S. Onari, R. Arita, H. Usui, Y. Tanaka, H. Kontani, and H. Aoki, Phys. Rev. Lett. **101**, 087004 (2008).
[10] Z. P. Yin, K. Haule, and G. Kotliar, Nat. Mater. **10**, 932 (2011).
[11] B. C. Sales, A. S. Sefat, M. A. McGuire, R. Y. Jin, D. Mandrus, and Y. Mozharivskyj, Phys. Rev. B **79**, 094521 (2009).
[12] Y. Mizuguchi, F. Tomioka, S. Tsuda, T. Yamaguchi, and Y. Takano, Appl. Phys. Lett. **94**, 012503 (2009).
[13] E. E. Rodriguez, Z. Zavalij, P. Y. Hsieh, and M. A. Green, J. Am. Chem. Soc. **132**, 10006 (2010).
[14] N. Tsyrulin, R. Viennois, E. Gianini, M. Boehm, M. Jimenez-Ruiz, A. A. Omrani, B. D. Piazza, and H. M. Ronnow, New. J. Phys. **14**, 073025 (2012).
[15] E. E. Rodriguez, C. Stock, P. Y. Hsieh, N. P. Butch, J. Paglione, and M. A. Green, Chem. Sci. **2**, 1782 (2011).
[16] C. Stock, E. E. Rodriguez, and M. A. Green, Phys. Rev. B **85**, 094507 (2012).
[17] E. E. Rodriguez, C. Stock, P. Zajdel, K. L. Krycka, C. F. Majkrzak, P. Zavalij, and M. A. Green, Phys. Rev. B **84**, 064403 (2011).
[18] C. Koz, S. Rossler, A. A. Tsirlin, S. Wirth, and U. Schwarz, Phys. Rev. B **88**, 094509 (2013).
[19] S. Rossler, D. Cherian, W. Lorenz, M. Doerr, C. Koz, C. Curfs, Y. Prots, U. K. Rossler, U. Schwarz, S. Elizabeth, and S. Wirth, Phys. Rev. B **84**, 174506 (2011).
[20] Y. Mizuguchi, K. Hamada, K. Goto, H. Takatsu, H. Kadowaki, and O. Miura, Solid State Commun. **152**, 1047 (2012).
[21] I. A. Zaliznyak, Z. J. Xu, J. S. Wen, J. M. Tranquada, G. D. Gu, V. Solovyov, V. N. Glazkov, A. I. Zheludev, V. O. Garlea, and M. B. Stone, Phys. Rev. B **85**, 085105 (2012).
[22] E. E. Rodriguez, D. A. Sokolov, C. Stock, M. A. Green, O. Sobolev, J. A. Rodriguez-Rivera, H. Cao, and A. Daoud-Aladine, Phys. Rev. B **88**, 165110 (2013).
[23] G. F. Chen, Z. G. Chen, J. Dong, W. Z. Hu, G. Li, X. D. Zhang, P. Zheng, J. L. Luo, and N. L. Wang, Phys. Rev. B **79**, 140509 (2009).
[24] See Supplemental Material at http://link.aps.org/supplemental/10.1103/PhysRevB.90.121113 for further experimental details, spectrometer calibration, detailed measurements of the *c*-axis dispersion, and separation of phonons from the magnetic cross section.
[25] J. A. Rodriguez, D. M. Adler, P. C. Brand, C. Broholm, J. C. Cook, C. Brocker, R. Hammond, Z. Huang, P. Hundertmakr, J. W. Lynn, N. C. Maliszewskyj, J. Moyer, J. Orndorff, D. Pierce, T. D. Pike, G. Scharfstein, S. A. Smee, and R. Vilaseca, Meas. Sci. Technol. **19**, 034023 (2008).
[26] H. F. Fong, B. Keimer, D. Reznik, D. L. Milius, and I. A. Aksay, Phys. Rev. B **54**, 6708 (1996).
[27] C. Stock, E. E. Rodriguez, M. A. Green, P. Zavalij, and J. A. Rodriguez-Rivera, Phys. Rev. B **84**, 045124 (2011).
[28] P. J. Brown, *International Tables of Crystallography* (Kluwer, Dordrecht, 2006), Vol. C .
[29] O. J. Lipscombe, G. F. Chen, C. Fang, T. G. Perring, D. L. Abernathy, A. D. Christianson, T. Egami, N. Wang, J. Hu, and P. Dai, Phys. Rev. Lett. **106**, 057004 (2011).
[30] M. D. Lumsden, A. D. Christianson, E. A. Goremychkin, S. E. Nagler, H. A. Mook, M. B. Stone, D. L. Abernathy, T. Guidi, G. J. Macdougall, C. Cruz, A. S. Sefat, M. A. Mcguire, B. C. Sales, and D. Mandrus, Nat. Phys. **6**, 182 (2010).
[31] C. Stock, R. A. Cowley, W. J. L. Buyers, C. D. Frost, J. W. Taylor, D. Peets, R. Liang, D. Bonn, and W. N. Hardy, Phys. Rev. B **82**, 174505 (2010).
[32] K. Sugimoto, Z. Li, E. Kaneshita, K. Tsutsui, and T. Tohyama, Phys. Rev. B **87**, 134418 (2013).
[33] R. Coldea, S. M. Hayden, G. Aeppli, T. G. Perring, C. D. Frost, T. E. Mason, S. W. Cheong, and Z. Fisk, Phys. Rev. Lett. **86**, 5377 (2001).
[34] C. Stock, R. A. Cowley, W. J. L. Buyers, R. Coldea, C. L. Broholm, C. D. Frost, R. J. Birgeneau, R. Liang, D. A. Bonn, and W. N. Hardy, Phys. Rev. B **75**, 172510 (2007).
[35] S. O. Diallo, V. P. Antropov, T. G. Perring, C. Broholm, J. J. Pulikkotil, N. Ni, S. L. Budko, P. C. Canfield, A. Kreyssig, A. I. Goldman, and R. J. McQueeney, Phys. Rev. Lett. **102**, 187206 (2009).
[36] J. Zhao, D. T. Adroja, D. X. Yao, R. I. Bewley, S. Li, X. F. Wang, G. Wu, X. H. Chen, J. Hu, and P. Dai, Nat. Phys. **5**, 555 (2009).
[37] C. Lester, J. H. Chu, J. G. Analytis, T. G. Perring, I. R. Fisher, and S. M. Hayden, Phys. Rev. B **81**, 064505 (2010).
[38] M. Ramazanoglu, J. Lamsal, G. S. Tucker, J. Q. Yan, S. Calder, T. Guidi, T. Perring, R. W. McCallum, T. A. Lograsso, A. Kreyssig, A. I. Goldman, and R. J. McQueeney, Phys. Rev. B **87**, 140509 (2013).
[39] S. O. Diallo, D. K. Pratt, R. M. Fernandes, W. Tian, J. L. Zarestky, M. Lumsden, T. G. Perring, C. L. Broholm, N. Ni, S. L. Bud'ko, P. C. Canfield, H. F. Li, D. Vaknin, A. Kreyssig, A. I. Goldman, and R. J. McQueeney, Phys. Rev. B **81**, 214407 (2010).
[40] G. S. Uhrig, K. P. Schmidt, and M. Gruninger, Phys. Rev. Lett. **93**, 267003 (2004).
[41] E. W. Carlson, D. X. Yao, and D. K. Campbell, Phys. Rev. B **70**, 064505 (2004).
[42] J. Zhao, Y. Shen, R. J. Birgeneau, M. Gao, Z. Y. Lu, D. H. Lee, X. Z. Lu, H. J. Xiang, D. L. Abernathy, and Y. Zhao, Phys. Rev. Lett. **112**, 177002 (2014).
[43] W. Jayasekara, Y. Lee, A. Pandey, G. S. Tucker, A. Sapkota, J. Lamsal, S. Calder, D. L. Abernathy, J. L. Niedziela, B. N. Harmon, A. Kreyssig, D. Vaknin, D. C. Johnston, A. I. Goldman, and R. J. McQueeney, Phys. Rev. Lett. **111**, 157001 (2013).
[44] H. Tsunetsugu and M. Arikawa, J. Phys. Soc. Jpn. **75**, 083701 (2006).
[45] A. Lauchli, F. Mila, and K. Penc, Phys. Rev. Lett. **97**, 087205 (2006).
[46] B. A. Ivanov and A. K. Kolezhuk, Phys. Rev. B **68**, 052401 (2003).
[47] R. M. Fernandes, A. V. Chubukov, and J. Schmalian, Nat. Phys. **10**, 97 (2014).

[48] M. Tsuchiizu, Y. Ohno, S. Onari, and H. Kontani, Phys. Rev. Lett. **111**, 057003 (2013).
[49] Y. Ohno, M. Tsuchiizu, S. Onari, and H. Kontani, J. Phys. Soc. Jpn. **82**, 013707 (2013).
[50] C. Stock, W. J. L. Buyers, R. Liang, D. Peets, Z. Tun, D. Bonn, W. N. Hardy, and R. J. Birgeneau, Phys. Rev. B **69**, 014502 (2004).
[51] G. Shirane, S. M. Shapiro, and J. M. Tranquada, *Neutron Scattering with a Triple Axis Spectrometer* (Cambridge University Press, Cambridge, UK, 2002).
[52] H. F. Fong, P. Bourges, Y. Sidis, L. P. Regnault, J. Bossy, A. Ivanov, D. L. Milius, I. A. Aksay, and B. Keimer, Phys. Rev. B **61**, 14773 (2000).
[53] P. Dai, H. A. Mook, R. D. Hunt, and F. Dogan, Phys. Rev. B **63**, 054525 (2001).
[54] G. Xu, Z. Xu, and J. M. Tranquada, Rev. Sci. Instrum. **84**, 083906 (2013).
[55] N. B. Christensen, D. F. McMorrow, H. M. Ronnow, B. Lake, S. M. Hayden, G. Aeppli, T. G. Perring, M. Mangkorntong, M. Nohara, and H. Tagaki, Phys. Rev. Lett. **93**, 147002 (2004).
[56] J. M. Tranquada, H. Woo, T. G. Perring, H. Goka, G. D. Gu, G. Xu, M. Fujita, and K. Yamada, Nature (London) **429**, 534 (2004).
[57] D. Reznik, J.-P. Ismer, I. Eremin, L. Pintschovius, T. Wolf, M. Arai, Y. Endoh, T. Masui, and S. Tajima, Phys. Rev. B **78**, 132503 (2008).
[58] C. Stock, W. J. L. Buyers, R. A. Cowley, P. S. Clegg, R. Coldea, C. D. Frost, R. Liang, D. Peets, D. Bonn, W. N. Hardy, and R. J. Birgeneau, Phys. Rev. B **71**, 024522 (2005).
[59] A. T. Boothroyd, P. Babkevich, D. Prabhakaran, and P. G. Freeman, Nature (London) **471**, 341 (2011).
[60] H. Ulbrich, P. Steffens, D. Lamago, Y. Sidis, and M. Braden, Phys. Rev. Lett. **108**, 247209 (2012).
[61] S. Chi, J. A. Rodriguez-Rivera, J. W. Lynn, C. Zhang, D. Phelan, D. K. Singh, R. Paul, and P. Dai, Phys. Rev. B **84**, 214407 (2011).
[62] Z. Xu, J. Wen, Y. Zhao, M. Matsuda, W. Ku, X. Liu, G. Gu, D. H. Lee, R. J. Birgeneau, J. M. Tranquada, and G. Xu, Phys. Rev. Lett. **109**, 227002 (2012).
[63] H. Luo, R. Zhang, M. Laver, Z. Yamani, M. Wang, X. Lu, M. Wang, Y. Chen, S. Li, S. Chang, J. W. Lynn, and P. Dai, Phys. Rev. Lett. **108**, 247002 (2012).
[64] R. Khasanov, M. Bendele, A. Amato, P. Babkevich, A. T. Boothroyd, A. Cervellino, K. Conder, S. N. Gvasaliya, H. Keller, H. H. Klauss, H. Luetkens, V. Pomjakushin, E. Pomjakushina, and B. Roessli, Phys. Rev. B **80**, 140511 (2009).
[65] C. Cao, P. J. Hirschfeld, and H. P. Cheng, Phys. Rev. B **77**, 220506 (2008).
[66] F. Krüger, S. Kumar, J. Zaanen, and J. van den Brink, Phys. Rev. B **79**, 054504 (2009).
[67] H. Gretarsson, S. R. Saha, T. Drye, J. Paglione, J. Kim, D. Casa, T. Gog, W. Wu, S. R. Julian, and Y. J. Kim, Phys. Rev. Lett. **110**, 047003 (2013).
[68] A. M. Turner, F. Wang, and A. Vishwanath, Phys. Rev. B **80**, 224504 (2009).
[69] K. Haule and G. Kotliar, New J. Phys. **11**, 025021 (2009).
[70] R. A. Ewings, T. G. Perring, R. I. Bewley, T. Guidi, M. J. Pitcher, D. R. Parker, S. J. Clarke, and A. T. Boothroyd, Phys. Rev. B **78**, 220501 (2008).
[71] B. Schmidt, M. Siahatgar, and P. Thalmeier, Phys. Rev. B **81**, 165101 (2010).
[72] E. E. Rodriguez, C. Stock, K. L. Krycka, C. F. Majkrzak, P. Zajdel, K. Kirshenbaum, N. P. Butch, S. R. Saha, J. Paglione, and M. A. Green, Phys. Rev. B **83**, 134438 (2011).
[73] D. G. Free and J. S. O. Evans, Phys. Rev. B **81**, 214433 (2010).
[74] J. X. Zhu, R. Yu, H. Wang, L. L. Zhao, M. D. Jones, J. Dai, E. Abrahams, E. Morosan, M. Fang, and Q. Si, Phys. Rev. Lett. **104**, 216405 (2010).
[75] E. E. McCabe, C. Stock, E. E. Rodriguez, A. S. Wills, J. W. Taylor, and J. S. O. Evans, Phys. Rev. B **89**, 100402(R) (2014).
[76] J. Zhao, H. Cao, E. Bourret-Courchesne, D. H. Lee, and R. J. Birgeneau, Phys. Rev. Lett. **109**, 267003 (2012).
[77] I. A. Zaliznyak, Z. Xu, J. M. Tranquada, G. Gu, A. M. Tsvelik, and M. B. Stone, Phys. Rev. Lett. **107**, 216403 (2011).
[78] Z. P. Yin, K. Haule, and G. Kotliar, arXiv:1311.1188.
[79] J. Chaloupka and G. Khaliullin, Phys. Rev. Lett **110**, 207205 (2013).
[80] Y.-J. Kim, A. P. Sorini, C. Stock, T. G. Perring, J. van den Brink, and T. P. Devereaux, Phys. Rev. B **84**, 085132 (2011).
[81] R. A. Cowley, W. J. L. Buyers, C. Stock, Z. Yamani, C. Frost, J. W. Taylor, and D. Prabhakaran, Phys. Rev. B **88**, 205117 (2013).
[82] J. P. Hill, G. Blumberg, Y.-J. Kim, D. S. Ellis, S. Wakimoto, R. J. Birgeneau, S. Komiya, Y. Ando, B. Liang, R. L. Greene, D. Casa, and T. Gog, Phys. Rev. Lett. **100**, 097001 (2008).
[83] J. D. Perkins, R. J. Birgeneau, J. M. Graybeal, M. A. Kastner, and D. S. Kleinberg, Phys. Rev. B **58**, 9390 (1998).
[84] C. Stock, R. A. Cowley, J. W. Taylor, and S. M. Bennington, Phys. Rev. B **81**, 024303 (2010).